# Platform Tolerant and Conformal RFID Tag Antenna: Design, Construction and Measurements

**Harish Rajagopalan and Yahya Rahmat-Samii**

Electrical Engineering Department
University of California at Los Angeles
Los Angeles, CA, 90095-1594, USA
harish@ee.ucla.edu, rahmat@ee.ucla.edu

***Abstract*—** This paper presents the design of a novel platform tolerant and conformal RFID (Radio Frequency Identification) tag antenna, which operates at the 902–928 MHz UHF band. The antenna has a simple, low-profile (1.8 mm thick) structure. It consists of two microstrip patches, which are separated by a narrow gap and driven by a microchip in the gap. The tag is designed to complex conjugate match an Alien-Higgs2 microchip. The performance of the tag is investigated on different surfaces (free space, human and metal) through simulations using parameters like power reflection coefficient, input impedance and radiation patterns. The effects of bending are investigated on the tag design. Experimental read-range, radiation pattern and impedance measurements are performed for the tag. High Frequency Structure Simulator (HFSS) simulation validation has been achieved due to excellent agreement with measurements for this particular application. The experimental measurements show that the maximum boresight average read range of the designed RFID tag on different platforms is about 3.5m (4 W EIRP).

***Index Terms*—** Conformal, metal, RFID, tag.

## I. INTRODUCTION

Radio frequency identification (RFID) systems have attracted considerable attention in recent years. These systems have become very popular in applications like asset identification, inventory management and human monitoring [1, 2]. In processes like supply chain management, the RFID tags can keep a track of the products throughout the supply course assembly chain [3]. RFID tags in the form of an implantable chip [4] or wrist-bands [5] can be used to track the movement of people in different environments (like hospitals). Due to the non line-of sight operation, larger read range and ability to store more information, RFID tags serve as a possible replacement to bar codes [6]. A typical RFID system consists of a reader and a tag where the tag is a passive device consisting of an antenna and a microchip. Near-field (13.56 MHz) RFID systems work on the principle of inductive coupling between the reader and the tag [7]. Far-field (915 MHz, 2.4GHz) RFID tags work on the principle of traveling waves between the reader and the tag [8, 9]. The UHF (860–960 MHz) band is of particular interest due to the long read range possibility and low manufacturing costs. These RFID systems operate at various frequency bands around the world (902–928 MHz in North and South America).

Passive UHF RFID tags are attached to the required object for tagging purposes. At the UHF frequency, high-dielectric (human) or high-conductivity (metal) objects degrade the performance of the tag affecting the tag impedance, ability to couple power to the microchip and the read range of the tag. These RFID tag problems are well documented in [10, 11]. Various metal-mountable tag designs have been proposed in literature [12–14]. Slim tag with vias designed on high-impedance surface [15], tag on a lossy substrate with a stacked structure [16] and small loop tag [17] are some other examples of metal mountable tags where the tag antennas are designed such that the tag antenna parameters like frequency, efficiency, bandwidth, radiation pattern and input impedance do not undergo severe degradation on metal. Platform-tolerant tag designs have also been proposed where the tag demonstrates stable performance on different surfaces [18].

Technological progress in RFID readers and tags enables new and interesting applications and more efficient ways of using current systems. The design of the antenna is a critical part of the RFID tag design [19]. A number of challenges have to be addressed while developing RFID antennas which include simple design for low cost mass production (as bar code are much cheaper than tags at present), reliable performance in free space and on different surfaces, low profile structure and structural conformality (for nonplanar objects). Most of the tag designs in literature answer some of these challenges [20–22]. Therefore, there is a need to develop new RFID tag antenna designs which successfully deal with all the challenges presented. Large demand still exists in the market for UHF band disposal, multipurpose RFID tags. Good, practical solutions are still missing.

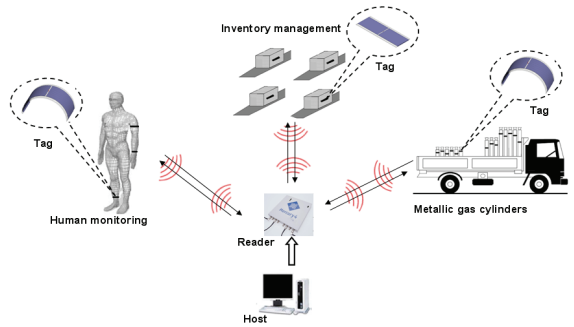


Fig. 1. Potential security and safety applications of the proposed RFID tag.

In this paper, we propose the design of a novel UHF RFID tag which operates in the US (902–928 MHz) band. The low profile unique design makes the tag ideal for low cost mass production (no via structure). The tag operates on different surfaces making it platform tolerant. The tag also operates on non planar surfaces. This RFID tag antenna is designed to match the Alien Higgs-2 microchip. Firstly, the planar version of the tag is discussed in detail, both in free space and on metal plate. Impedance and pattern measurements are performed for the planar tag. After the successful investigation of the planar tag, the tag is conformed to study effects of structural bending on the tag performance. This conformal tag is then placed on different surfaces (human, metal) and through simulations the power reflection coefficient, input impedance and radiation patterns are investigated to study the effects of these surfaces on the tag performance. Finally, read-range measurements are performed using both planar and conformal tags in different environments. Initial investigations show that this tag can be used for both security and safety applications such as inventory control and reporting of high risk materials, gas cylinder movement and tracking, and human monitoring as shown in Fig. 1.

## II. TAG ANTENNA DESIGN

The goal of tag antenna is to maximize the detection range of the RFID tag. The antenna input impedance has to be conjugate matched to the microchip impedance to ensure maximum power transmission to the microchip. The power reflection coefficient between the antenna and the microchip is given by

$$\rho = 1 - \tau = 1 - \frac{4R_a R_{mc}}{\left|Z_a + Z_{mc}\right|^2}, \qquad (1)$$

where ρ is the power reflection coefficient, $\tau$ is the power transmission coefficient and $Z_a = R_a + jX_a$ and $Z_{mc} = R_{mc} + jX_{mc}$ are the complex antenna and microchip input impedances, respectively [1]. The antenna is designed to conjugate match to a microchip, Alien Higgs-2, which has an input parallel resistance of 1500 Ω and a capacitance of 1.2 pF (at 915 MHz, the microchip impedance is 14 – j145 Ω) as shown in Fig. 2.

Figure 2 shows the design of the planar RFID tag antenna. The tag antenna consists of two quarter-wave microstrip patches shorted to the ground plane by the shorting plates. These patches are placed next to each other separated by a gap and connected by a microchip in the feed location. The patches are placed on a thin FR-4 substrate ($\varepsilon_r$ = 4.4 and tanδ = 0.02) and foam layer backed by a ground plane (116mm x 40mm). The reason for choosing a thin FR-4 layer is that the FR-4 can be potentially replaced by paper substrate to form a green tag. The structure is simulated with High Frequency Structure Simulator (HFSS). The tag

dimensions are chosen such that it can operate both in free space and on metal and satisfy the condition: minimum -3dB half power bandwidth. To study the effect of metal plate, the tag is placed on a 250mm x 250mm x 2mm (approximately 0.9λ x 0.9λ x 0.006λ at 915 MHz) copper metal plate. The power reflection coefficient, input impedance, and radiation patterns are compared for the planar tag in free space and on metal ground plane to better understand the working of the tag.

The matching frequency (corresponds to the minimum value of power reflection coefficient in dB) is tuned by adjusting the patch length and gap width. The matching frequency decreases when the patch length is increased and it increases when the gap width is increased. The foam layer is used to improve bandwidth and radiation efficiency. The input resistance of the tag is controlled by changing the patch width (resistance increases when the patch width is reduced). The tag ground plane width is chosen such that the tag can satisfy the -3dB criteria for both free space and on metal.

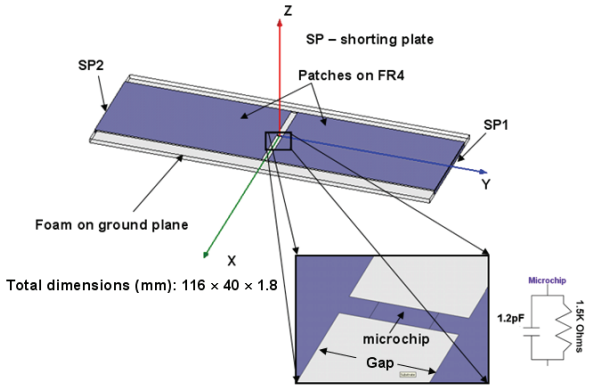


Fig. 2. Design of the RFID tag antenna.

The microchip has variable impedance over the frequency band and tag parameters are optimized taking this fact into consideration. Once the input impedance of the tag and the microchip are obtained, these values are inserted into eq. (1) to obtain power reflection coefficient. Figure 3 shows the power reflection coefficient calculated from the input impedance and the Alien Higgs-2 chip impedance for both free space and on metal. The optimized total dimensions of the tag are 40mm × 116mm × 1.8mm. Individual dimensions are as follows: patch–30mm x 57mm, Fr-4 substrate–30mm x 116mm x 0.4mm, foam substrate–30mm x 116mm x 0.4mm, shorting plate–30mm x 1.8mm, ground plane–40mm x 116mm and gap width–2mm.

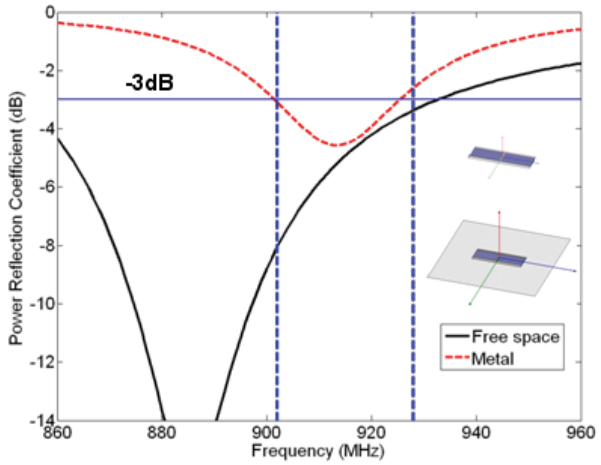


Fig. 3. Power reflection coefficient calculated from the antenna and the microchip impedance. The 902–928 MHz band is marked by two vertical lines.

Figure 4(a) shows the simulated input impedance when the optimized tag antenna is in free space. It can be clearly seen that the antenna resonance occurs close to 1100MHz (length of the antenna 116mm ~ λg/2). The operating region of the tag is marked with dotted lines. Figure 4(b) shows the input impedance (both real and imaginary part) of the tag in free space and on a 250mm x 250mm x 2mm copper plate. It can be seen that there is a change in the input impedance when the tag is placed on metal. Therefore, the tag is optimized to work well in free space and on metal plate. The input impedance of the tag at 915 MHz in free space and on metal is 32.9 + j167.8 and 3.7 + j147.9, respectively.

Figure 5(a) shows the change in power reflection coefficient for gap width variation. It can be seen that when all other design parameters are fixed to optimum values and the gap width is varied, the matching frequency increases significantly as the gap width increases for both free space and metal plate case. Figure 5(b) shows the effect of different size ground planes on the

tag performance. It can be seen that when all other design parameters are fixed to optimum values and the ground plane size is varied (thickness of ground plane fixed at 2mm), the matching frequency satisfies the -3dB condition over the entire band showing the robustness of the tag to metal attachment.

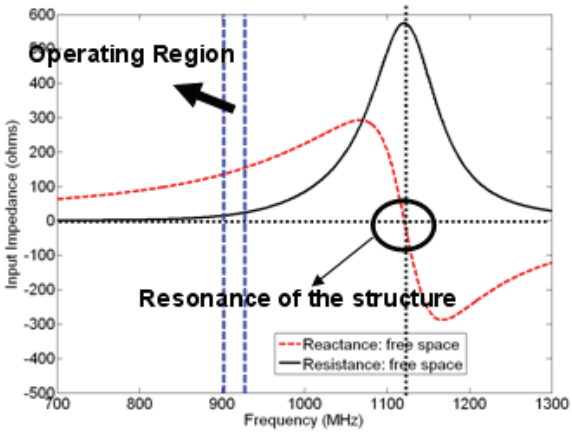


(a)

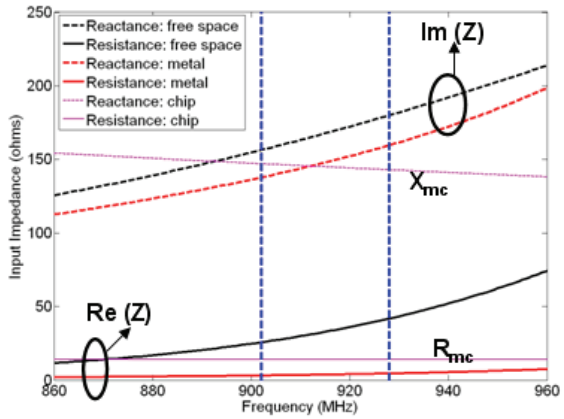


(b)

Fig. 4. Simulated input impedance of the antenna. (a) In free space. (b) In free space and on a 250mm x 250mm x 2mm copper plate. The 902–928 MHz band is marked by two vertical lines.

Complex interactions of currents and fields due to the antenna structure cause the tag to operate in a large loop-patch hybrid mode. From the current distribution view point, the tag appears to act in patch mode and from radiation pattern view point, the tag appears to operate in large loop mode (circumference of the loop is approximately 1λ at 915MHz). Figure 6(a) shows the current distribution on the top surface of the patches and ground plane for the planar tag in free space at 915 MHz. It is clear that the currents are maximum at the edges and minimum at the center of the tag (emulating a quarter-wave patch). The direction of current flow on the ground plane is in the opposite direction to the current on the top patch surface.

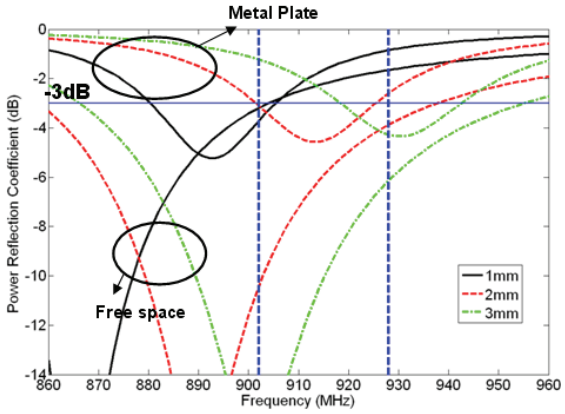


(a)

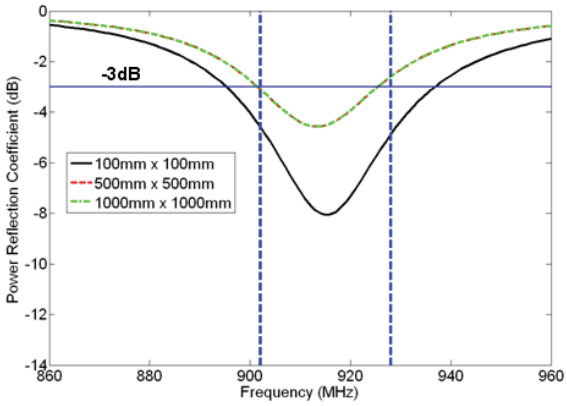


(b)

Fig. 5. Power reflection coefficient (a) Gap width variation. (b) Ground plane size variation.

Figure 6(b) shows the electric field distribution in the 0.4mm thick FR-4 substrate and the 1.4mm thick foam layer for the planar tag in free space at 915 MHz. The fields are maximum at the center. The fields are in the $+z$ direction on one patch and in the $-z$ direction on the other patch. Across the gap, the fields point in the $+y$ direction (horizontal electric field across the gap radiates).

## III. IMPEDANCE AND RADIATION PATTERN MEASUREMENTS

Extensive measurements were performed on the planar tag both in free space and on metal

plate. A prototype planar tag antenna was built and its input impedance and radiation patterns were measured.

### A. Impedance Measurements

Input impedance measurement of the tag is crucial as it helps to optimize the tag performance and improve its modelling in simulations. Due to a balanced structure, the impedance of the dual-patch microstrip antenna cannot be measured directly with a network analyzer. This is because the feed points of the balanced antenna should be driven by equal and opposite currents, which is not true if the antenna is connected to an unbalanced coax port of the network analyzer. In order to measure the input impedance of this antenna, a quarter-wave balun was designed with the center frequency at 915MHz. Fig. 7 shows the prototype antenna and the balun used for impedance measurements.

Suitable scheme is applied to calibrate the balun out of the measurement. The impedance measurement was done in free space, i.e., when the tag was placed on a low-permittivity polystyrene support, and also when the tag was placed on a 250mm × 250 mm x 2mm copper plate. The measurements were carried out in an anechoic chamber to ensure stable distortion-free conditions. Figure 8 shows the measured input impedance of the planar tag both in free space and on metal. Figure 8(a) shows the comparison of the input impedance between simulation and measurement in free space. Both the real and the imaginary part of the input impedance measured data follow the simulation curves very closely (in the band of operation). Figure 8(b) shows the comparison of the input impedance between simulation and measurement when the tag is placed on a metal plate. The measurements show the decrease in the real part as predicted from the simulation. There is very good agreement between the measured and simulated data. The difference at higher frequencies for the resistive part may be caused due to the balun-tag coupling and the balun bandwidth limitation.

### B. Radiation Pattern Measurements

Radiation pattern measurements were performed in the UCLA far-field anechoic chamber placing the tag on a polystyrene support and rotating it by an antenna positioner. Mercury4 reader with M/A-COM Dual antenna (5.9dBi gain) was used for reading the tag with single frequency operation at 915MHz (shown in Fig. 14(a)). The reader was controlled by a host computer. The maximum transmitted power was 4 W EIRP (for the US band). The minimum transmitted power required for reading the tag was determined at each measurement angle and the normalized radiation pattern was computed. Figure 9 shows the measurement setup and the normalized measured radiation pattern in the two principal planes when the tag is in free space and when the tag is plate on a metal plate. The peak

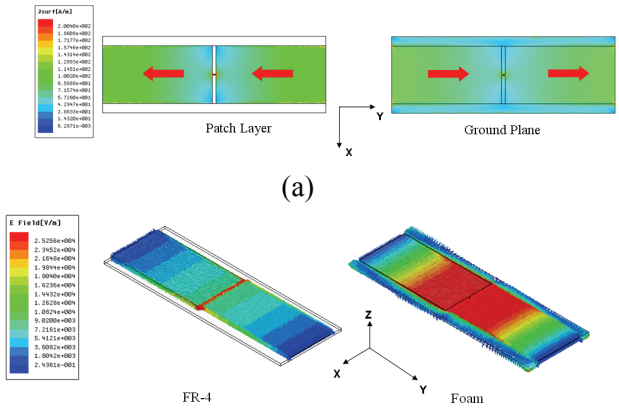


Fig. 6. (a) Surface currents on the planar tag in free space at 915 MHz. (b) Electric field distribution for the planar tag in free space at 915 MHz.

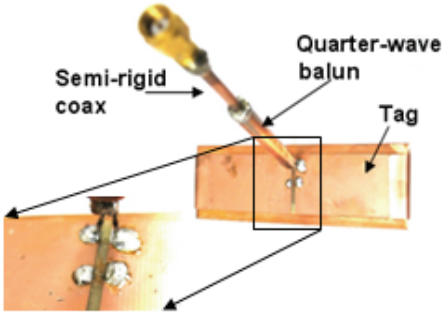


Fig. 7. Quarter-wave balun soldered to the prototype tag.

simulated directivity for the tag in free space and on metal plate are 3.53dB and 6.86dB at 915 MHz. All the patterns are normalized to their respective maximum values. The tag and the

reader were placed in the anechoic at a distance of 2m (far-field region of the reader antenna). The reader power was incremented in steps of 0.1dBm to find the minimum transmitted RF signal required to activate the tag. This activation was based on the criterion that the back-scattered modulated signal from the tag should be read continuously for 90 seconds. The positioner was rotated in steps of 5°.

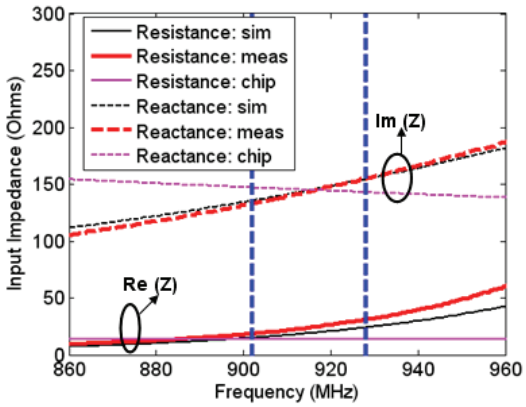


(a)

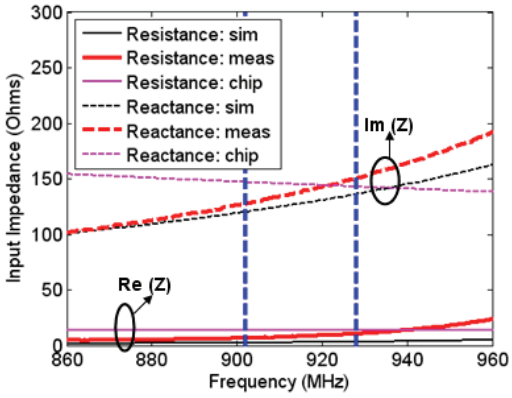


(b)

Fig. 8. Input impedance measurement (a) Free space. (b) Metal plate. The 902–928 MHz band is marked by two vertical lines.

Figure 9(b) shows the simulated and measured patterns for the tag in the *xz*-plane in both free space and on metal at 915 MHz. It can be seen that in free space the tag has omnidirectional pattern and on metal the tag is more directive with a small back lobe (present due to diffraction from the metallic plate edges). Due to the nature of the operating mechanism which involves both folded-dipole and patch characteristics, the pattern is omnidirectional in the *xz*-plane and Fig. 8 in the *yz*-plane (loop like pattern in both planes). Figure 9(c) shows the simulated and measured patterns for the tag in the *yz*-plane in both free space and on metal at 915 MHz. It can be seen that in free space the tag has a figure-8 pattern and on metal the tag has a broader pattern than in the xz-plane. The measured patterns follow the simulated patterns very closely in free space in both planes.

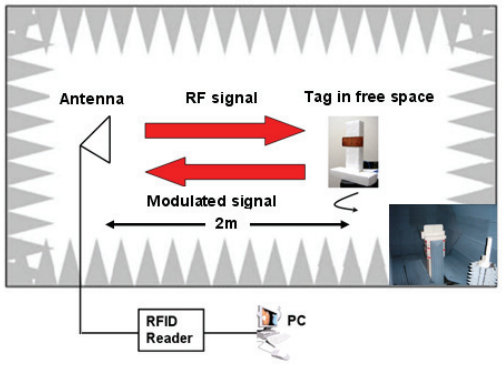


(a)

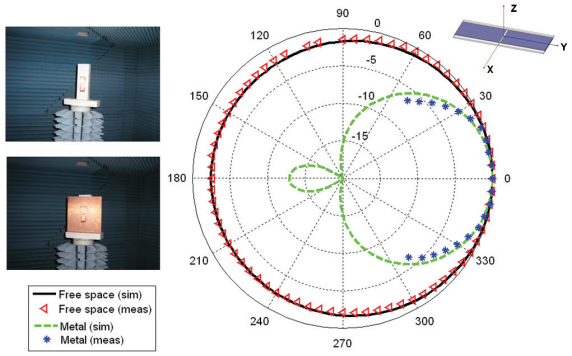


(b)

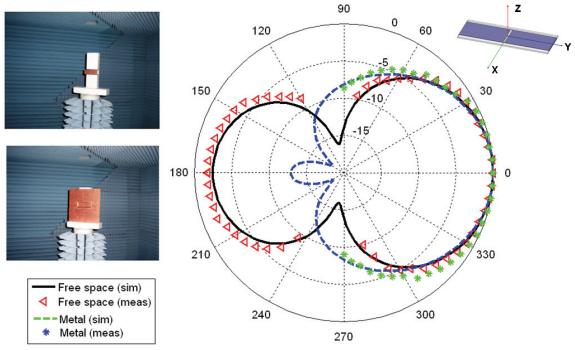


(c)

Fig. 9. (a) Radiation pattern measurement setup. (b) Normalized measured and simulated radiation pattern in the *XZ*-plane (Φ = 0°). (c) Normalized measured and simulated radiation pattern in the *YZ*-plane (Φ = 90°).The antenna is in free space and on a 250 mm × 250mm x 2mm copper plate. The scale is in dB.

On metal, the measured patterns follow the simulated patterns closely in both planes up to certain angles. At large angles, due to reader power limitations, the received power was too low to activate the tag. All the patterns are normalized to their maximum value. The read range measurements for the planar tag will be discussed later. The excellent agreement between the measured and simulated results for both the tag input impedance and radiation pattern shows that commercial radio frequency (RF) computer aided-design (CAD) software can be successfully used for RFID-type applications.

## IV. BENDING EFFECTS ON THE TAG

Once the planar design was investigated in detail, the tag was conformed in order to understand the effects of bending on the tag antenna performance.

Figure 10(a) shows the conformal tag in free space. The tag antenna is bent about a cylinder with radius of about 45mm. All the dimensions of the planar tag are kept constant. The input impedance of the tag at 915 MHz in planar and conformal form is 32.9 + j167.8 and 21.4 + j170.7, respectively. It can be seen that the input impedance for both planar and conformal forms of the tag are similar and the design is robust to conformality.

After understanding that bending does not appreciably affect the performance of the tag in free space, the conformal tag was mounted on different surfaces to study the effect of these surfaces on the antenna performance. The antenna was conformed around a metal cylinder (copper) as shown in Fig. 10(b). As shown in Fig. 10(c), the tag was also conformed around human model. The model is a typical representation of upper human arm (radius about 45mm). For simplicity, the human model was considered homogeneous (with dielectric constant of 58.8 and conductivity of 0.84S/m). Figure 11 shows that the input impedance of the tag does not change when placed on metal and human arm. The input impedance of the conformal tag at 915 MHz on metal cylinder and human arm is 4.1 + j150.7 and 6.7 + j151.47, respectively. Figure 12 shows the comparison of the power reflection coefficient between the planar and conformal tag and it can be seen that the bending does not change the performance significantly. Figure 12 also shows that the resonant frequency of the conformal tag does not change on different surfaces. It is also observed that the power reflection coefficient satisfies the half-power bandwidth for all the cases. Similar half-power bandwidth and input impedance characteristics were obtained when the tag was placed on multilayer human models as discussed in [2].

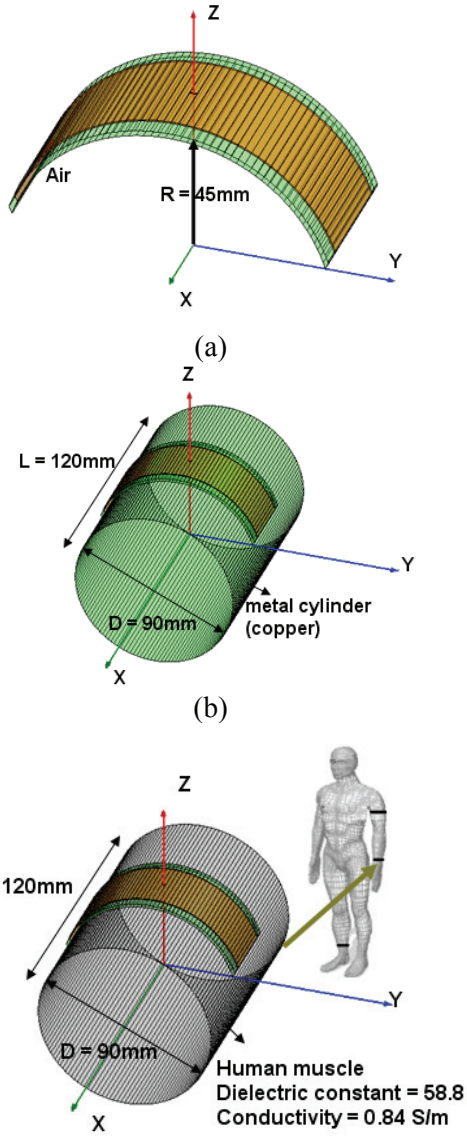


Fig. 10. (a) Conformal RFID tag design. (b) RFID conformal tag on metal cylinder. (c) RFID conformal tag on upper part of human arm.

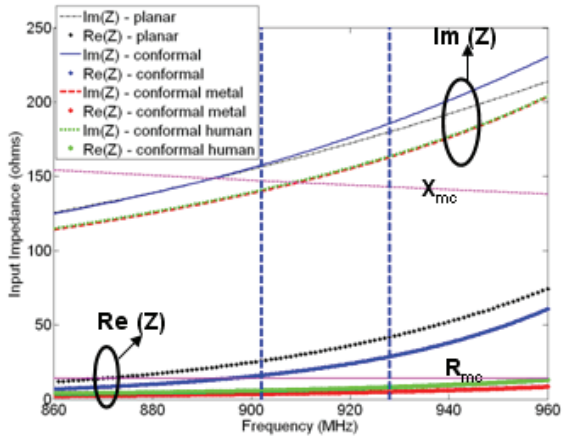


Fig. 11. Simulated input impedance of the antenna for the three cases described in Fig. 10. The 902–928 MHz band is marked by two vertical lines.

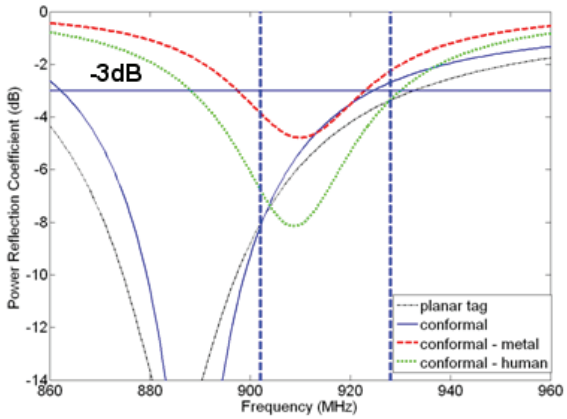


Fig. 12. Power reflection coefficient calculated for the simulated antenna input impedance and the Alien Higgs-2 microchip for the three cases described in Fig. 10. The 902–928 MHz band is marked by vertical lines.

Figure 13 shows the comparison of the radiation patterns (directivity in dB) between planar tag, conformal tag, conformal tag on metal and conformal tag on human arm in the xz-plane and yz-plane at 915 MHz. It is observed that the directivity slightly decreases for the bending case (conformal) with respect to planar tag but the patterns are similar. Figure 13 also shows that the radiation patterns are only slightly different in the xz-plane and yz-plane for metal cylinder and human arm case. It is also clear that when placed on metal cylinder, the directivity of the tag increases which is expected.

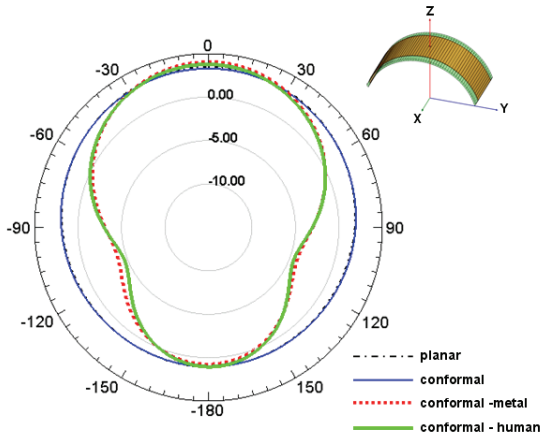


(a)

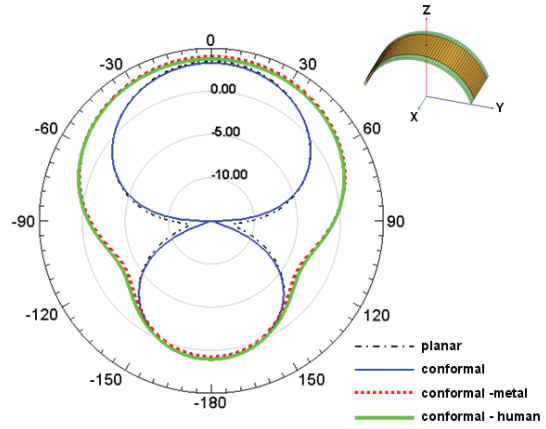


(b)

Fig. 13. Comparison between planar tag, conformal tag, conformal tag on metal and conformal tag on human arm. (a) Radiation pattern in the xz-plane (φ = 0°). (b) Radiation pattern in the yz-plane (φ = 90°).

## V. READ RANGE MEASUREMENTS

Typically, 2–5m read range is desired with passive UHF RFID systems. Read range measurements were conducted in an open environment to avoid reflections from surroundings at the single operating frequency of the reader (915MHz). The measurement setup is shown in Fig. 14(a). Microwave absorbers were placed on the floor to avoid ground reflections.

Figure 14(a) shows the reader antenna and central unit on a trolley (reader antenna dimensions were 230mm × 480mm). The maximum read range was defined as the maximum

line-of-sight distance from the reader antenna where the reader detects the tag continuously without interruption for 90 seconds. Once the tag is moved further from the maximum read range, it did not satisfy the criteria of continuous detection. The output power of the reader is fixed at 30.1dBm. The reader antenna gain is 5.9 dBi. The read range formula is given by

$$r_{\max} = d\sqrt{\frac{EIRP}{P_{\min} G_t L_c}} \quad , \qquad (2)$$

where $P_{min}$ is the minimum power required to communicate with the tag is recorded, $L_c$ is the loss of the connecting cable (1dB), $G_t$ is the gain of the transmitting antenna (5.9dBi), d is the distance of the reader to the tag and EIRP is effective isotropic radiated power (36dBm) [1].

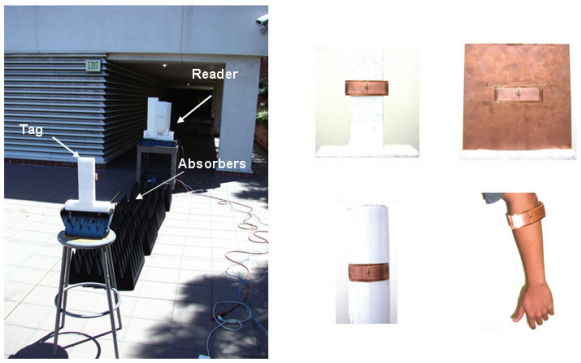


(a) (b)

Fig. 14. (a) Read range measurement setup. (b) The prototype tag on the polystyrene support in free space, on metal plate, on PVC cylinder and on human arm.

Figure 15 shows the plot of maximum measured boresight read range and the corresponding minimum power to activate the tag for both free space and on metal operation at 915MHz. The regression lines are drawn using equation (2) and fit well with measurements. Table I shows the maximum read range for the tag in free space and on different surfaces like flat metal plate, metal cylinder, human arm and lower part of human leg some of which are shown in Fig. 14(b) at the boresight direction. The reading distance remains fairly constant with an average boresight read range of about 3.5m on different platforms with the current reader configuration. The radiation efficiency of the tag is approximately 95% in free space, 60% on metal and about 50% on human arm model. The read range values differ for different platforms due to different matching (with chip impedance), directivity and radiation efficiencies. The structure is inherently less lossy (thin FR4 substrate) and it has a higher radiation resistance compared to small loop tags. Therefore, the tag has significantly better read range than the small loop tag [17].

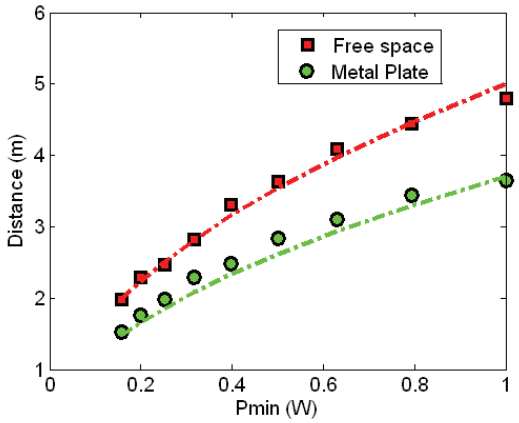


Fig. 15. Maximum measured boresight read range versus minimum power for tag in free space and on metal plate with best-fit curves.

Table 1: Maximum measured boresight read distance of the tag on different surfaces at 915MHz at 4W EIRP.

| | |
|---|---|
| On polystyrene support (free space) | 4.8m |
| On 250mm × 250mm x 2mm copper plate | 3.8 m |
| On PVC pipe (free space) – radius (50mm) | 4.5m |
| On metal cylinder – radius (50mm) | 3.9 m |
| On human arm | 3.5 m |
| On lower part of human leg | 3.4 m |
| On lower part of human leg (with clothing) | 3.4 m |

## VI. CONCLUSION

A simple, conformal, low-profile (1.8 mm) microstrip antenna suitable for RFID tags has been proposed. The tag is designed to conjugate match Alien-Higgs2 microchip impedance (14 – j145Ω at 915MHZ) and the tag operates at the 902–928 MHz UHF band. A prototype of the tag was built

and tested by measuring its input impedance and radiation pattern. The input impedance measurements were performed using balun approach due to the balanced geometry of the tag. Excellent agreement was achieved between the measured and HFSS simulated data for both input impedance and radiation pattern for the planar tag. The bending effects were studied for the tag and it was observed that the tag was robust to conformality. The conformal tag was then placed on different surfaces and through simulations it was observed that the tag performed well on all different surfaces. Read range measurements were performed for the tag in planar and conformal form on different surfaces and an average successful read range of about 3.5m was achieved (4W EIRP).

## ACKNOWLEDGMENT

The authors would like to thank Tomi Koskinen (post-doc visiting scholar from Finland) for the fruitful discussions. The authors would also like to thank Dr. Keisuke Noguchi (visiting professor from Japan) for his suggestions with the impedance measurements and Jeffrey Akamine (undergraduate student from UCLA) for helping with outdoor read range measurements.

## REFERENCES

[1] K. V. S. Rao, P. V. Nikitin, and S. F. Lam, "Antenna design for UHF RFID tags: A review and a practical application," *IEEE Transactions on Antennas and Propagation*, vol. 53, no. 12, pp. 3870–3876, Dec. 2005.

[2] G. Marrocco, "The art of UHF RFID antenna design: impedance-matching and size-reduction techniques," *IEEE Antennas and Propagation Magazine*, vol. 50, no. 1, pp. 66–79, Feb. 2008.

[3] R. Glidden et al. "Design of ultra-low-cost UHF RFID tags for supply chain applications," *IEEE Communications Magazine*, vol. 42, no. 8, pp. 140–151, Aug. 2004.

[4] K. R Foster and J. Jaeger, "RFID inside: The murky ethics of implanted chips," *IEEE Spectrum*, pp. 24–29, March 2007.

[5] L. Yang, L. J. Martin, D. Staiculescu, C. P. Wong, and M. M. Tentzeris, "Conformal Magnetic Composite RFID for Wearable RF and Bio-Monitoring Applications," *IEEE Transactions on Microwave Theory and Techniques,* vol. 56, no. 12, pp. 3223–3230, Dec. 2008.

[6] R. Weinstein, "RFID: a technical overview and its application to the enterprise," *IT Professional*, vol. 7, no. 3, pp. 27–33, May-June 2005.

[7] K. Myny, S. Van Winckel, S. Steudel, P. Vicca, S. De Jonge, M. J. Beenhakkers, C. W. Sele, N. A. J. van Aerle, G. H. Gelinck, J. Genoe, and P. Heremans, "An Inductively-Coupled 64b Organic RFID Tag operating at 13.56MHz with a Data Rate of 787b/s," *IEEE International Solid-State Circuits Conference*, pp. 290–614, Feb. 2008.

[8] G. Marrocco, "Gain-optimized self-resonant meander line antennas for RFID applications," *Antennas Wireless Propag. Lett.*, vol. 2, no. 21, pp. 302–305, 2003.

[9] Q. Xianming and Y. Ning, "A folded dipole antenna for RFID," *Proc. IEEE Antennas and Propagation Soc. Int. Symp.*, vol. 1, Jun. 2004, pp. 97–100.

[10] P. R. Foster and R. A. Burberry, "Antenna problems in RFID systems," *Proc. Inst. Elect. Eng. Colloquium RFID Technology*, pp. 3/1–3/5, Oct. 1999.

[11] D. M. Dobkin and S. M. Weigand, "Environmental effects on RFID tag antennas," *IEEE MTT-S International Microwave Symposium*, pp. 135–138, June 2005.

[12] B. Yu, S. -J. Kim, B. Jung, F. J. Harackiewicz, and B. Lee, "RFID tag antenna using two-shorted microstrip patches mountable on metallic objects," *Microwave and optical technology letters*, vol. 49, no. 2, pp. 414–416, Feb. 2007.

[13] M. Hirvonen, P. Pursula, K. Jaakkola, and K. Laukkanen, "Planar inverted-F antenna for radio frequency identification," *Electronics Letters,* vol. 40, no. 14, pp. 848–850, July 2004.

[14] K. H. Kim, J. G. Song, D. H. Kim, H. S. Hu, and J. H. Park, "Fork-shaped RFID tag antenna mountable on metallic surfaces," *Electronics Letters*, vol. 43, no. 25, pp. 1400–1402, Dec. 2007.

[15] S. -L. Chen and K. -H. Lin, "A Slim RFID Tag Antenna Design for Metallic Object Applications," *Antennas Wireless Propag. Lett.*, vol. 7, pp. 729–732, 2008.
[16] H. W. Son, "Design of RFID tag antenna for metallic surfaces using lossy substrate," *Electronics Letters*, vol. 44, no. 12, pp. 711–713, June 2005.
[17] M. L. Ng, K. S. Leong, and P. H. Cole, "A small passive UHF RFID tag for metallic item identification," *International Technical Conference on Circuits/Systems, Computers and Communications*, Jul. 2006.
[18] L. S. Chan, K. W. Leung, R. Mittra, K. V. S. Rao, "Platform-tolerant Design for an RFID Tag Antenna," *IEEE International Workshop on Anti-counterfeiting, Security, Identification,* pp. 57–60, April 2007.
[19] J. T. Prothro, "Improved performance of a Radio frequency identification tag antenna on a metal ground plane," *M.S. Thesis,* Georgia Institute of Technology, 2007.
[20] H. W. Son and C. S. Tyo, "Design of RFID Tag Antennas Using an Inductively Coupled Feed," *Electronics Letters*, vol. 41, no. 18, pp. 994-996, Sept. 2005.
[21] C. Cho, H. Choo and I. Park, "Design of Novel RF1ID Tag Antennas for Metallic Objects," *IEEE International Symposium on Antennas and Propagation Digest*, pp. 3245-3248, July 2006.
[22] N. Michishita and Y. Yamada, "A Novel Impedance Matching Structure for a Dielectric Loaded 0.05 Wavelength Small Meander Line Antenna," *IEEE International Symposium on Antennas and Propagation*, pp. 1347–1350, July 2006.

**Harish Rajagopalan** (S'03) received the B.E. degree from Government College of Engineering, Pune, India in Electronics and Telecommunications in August 2002, and M.S. degree from Auburn University, AL, USA in Electrical Engineering in June 2005. He is currently working toward the Ph.D. degree at University of California, Los Angeles (UCLA). He has worked in the Antenna Research, Analysis, and Measurement Laboratory at UCLA under the direction of Prof.Y. Rahmat-Samii since July of 2005. His research interests include charaterization of reflectarray elements, microstrip and reconfigurable antenna designs, bio-medical applications of electromagnetics and RFID systems.

**Yahya Rahmat-Samii** (S'73-M'75-SM'79-F'85) received the M.S. and Ph.D. degrees in electrical engineering from the University of Illinois, Urbana-Champaign.

He is a Distinguished Professor, holder of the Northrop Grumman Chair in Electromagnetics, and past Chairman of the Electrical Engineering Department, University of California, Los Angeles (UCLA). He was a Senior Research Scientist with the National Aeronautics and Space Administration (NASA) Jet Propulsion Laboratory (JPL), California Institute of Technology prior to joining UCLA in 1989. In summer 1986, he was a Guest Professor with the Technical University of Denmark (TUD). He has also been a consultant to numerous aerospace and wireless companies.

He has been Editor and Guest editor of numerous technical journals and books. He has authored and coauthored over 750 technical journal and conference papers and has written 25 book chapters. He is a coauthor of *Electromagnetic Band Gap Structures in Antenna Engineering* (New York: Cambridge, 2009), *Implanted Antennas in Medical Wireless Communications* (Morgan & Claypool Publishers, 2006), *Electromagnetic Optimization by Genetic Algorithms (New York: Wiley, 1999)*, and *Impedance Boundary Conditions in Electromagnetics* (New York: Taylor & Francis, 1995). He has received several patents. He has had pioneering research contributions in diverse areas of electromagnetics, antennas, measurement and diagnostics techniques, numerical and asymptotic methods, satellite and personal communications, human/antenna interactions, frequency selective

surfaces, electromagnetic band-gap structures, applications of the genetic algorithms and particle swarm optimization, etc., (visit http://www.antlab.ee.ucla.edu/).

Dr. Rahmat-Samii is a Fellow of the Institute of Advances in Engineering (IAE) and a member of Commissions A, B, J and K of USNC/URSI, the Antenna Measurement Techniques Association (AMTA), Sigma Xi, Eta Kappa Nu and the Electromagnetics Academy. He was Vice-President and President of the IEEE Antennas and Propagation Society in 1994 and 1995, respectively. He was appointed an IEEE AP-S Distinguished Lecturer and presented lectures internationally. He was a member of the Strategic Planning and Review Committee (SPARC) of the IEEE. He was the IEEE AP-S Los Angeles Chapter Chairman (1987-1989); his chapter won the best chapter awards in two consecutive years. He is listed in Who's Who in America, Who's Who in Frontiers of Science and Technology and Who's Who in Engineering. Professor Rahmat-Samii is the designer of the IEEE Antennas and Propagation Society (IEEE AP-S) logo displayed on all IEEE-AP-S publications. He has been the plenary and millennium session speaker at numerous national and international symposia. He has been the organizer and presenter of many successful short courses worldwide. He was a Directors and Vice President of AMTA for three years. He has been Chairman and Co-chairman of several national and international symposia. He was a member of the University of California at Los Angeles (UCLA) Graduate council for three years.

For his contributions, Dr. Rahmat-Samii has received numerous NASA and JPL Certificates of Recognition. In 1984, he received the Henry Booker Award from URSI, which is given triennially to the most outstanding young radio scientist in North America. Since 1987, he has been designated every three years as one of the Academy of Science's Research Council Representatives to the URSI General Assemblies held in various parts of the world. He was also invited speaker to address the URSI 75th anniversary in Belgium. In 1992 and 1995, he received the Best Application Paper Prize Award (Wheeler Award) for papers published in 1991 and 1993 IEEE Transactions on Antennas and Propagation. In 1999, he received the University of Illinois ECE Distinguished Alumni Award. In 2000, Prof. Rahmat-Samii received the IEEE Third Millennium Medal and the AMTA Distinguished Achievement Award. In 2001, Rahmat-Samii received an Honorary Doctorate in physics from the University of Santiago de Compostela, Spain. In 2001, he became a Foreign Member of the Royal Flemish Academy of Belgium for Science and the Arts. In 2002, he received the Technical Excellence Award from JPL. He received the 2005 URSI Booker Gold Medal presented at the URSI General Assembly. He is the recipient of the 2007 Chen-To Tai Distinguished Educator Award of the IEEE Antennas and Propagation Society. In 2008, he was elected to the membership of the National Academy of Engineering (NAE). In 2009, he was selected to receive the IEEE Antennas and Propagation Society highest award, Distinguished Achievement Award, for his outstanding career contributions. Prof. Rahmat-Samii is the designer of the IEEE AP-S logo which is displayed on all IEEE AP-S publications.